

Article type : Research Article

Biological evaluation the 2-aryl-2,3-dihydrobenzodiazaborinin-4(1*H*)-ones as potential dual α -glucosidase and α -amylase inhibitors with antioxidant properties

Malose J. Mphahlele,^{1*} Nontokozo M. Magwaza,¹ Sibusiso T. Malindisa² and Yee Siew Choong^{3*}

¹ Department of Chemistry, College of Science, Engineering and Technology, University of South Africa, Private Bag X06, Florida 1710, South Africa. E-mail: magwan@unisa.ac.za (NMM)

² Department of Life & Consumer Sciences, College of Agriculture and Environmental Sciences, University of South Africa, Private Bag X06, Florida 1710, South Africa. E-mail: malinst@unisa.ac.za (STM)

³ Institute for Research in Molecular Medicine (INFORMM), Universiti Sains Malaysia, Penang 11800, Malaysia

* Authors for correspondence: mphahmj@unisa.ac.za (MJM) and yeeseiw@usm.my (YSC)

Abstract: The 2-aryl-2,3-dihydrobenzodiazaborinin-4(1*H*)-ones (azaborininone) were synthesized as analogues of the 2-arylquinazoline-4(1*H*)-ones and screened through enzymatic assay *in vitro* for inhibitory effect against α -glucosidase and α -amylase activities. These azaborininones exhibited moderate to good inhibitory effect against these enzymes compared to acarbose used as a reference standard. The results are supported by the enzyme-ligand interactions through kinetics (*in vitro*) and molecular docking (*in silico*) studies. The test compounds also exhibited significant antioxidant activity through the 2,2-diphenyl-1-picrylhydrazyl (DPPH) and nitric oxide (NO) free radical scavenging assays. These azaborininone derivatives exhibited no effect on the viability of the human lung cancer (A549) cell line after 24 h, and were also not toxic towards the Vero cells.

This article has been accepted for publication and undergone full peer review but has not been through the copyediting, typesetting, pagination and proofreading process, which may lead to differences between this version and the [Version of Record](#). Please cite this article as [doi: 10.1111/CBDD.13893](https://doi.org/10.1111/CBDD.13893)

This article is protected by copyright. All rights reserved

Keywords: 2-Aryl-2,3-dihydrobenzodiazaborinin-4(1*H*)-ones; α -glucosidase; α -amylase; antioxidant; toxicity; drug-receptor interactions

1. Introduction

The synthesis of boron-based heteroaromatic compounds has fascinated synthetic chemists for some time to understand their aromaticity, and to expand molecular diversity particularly through developments in the Suzuki–Miyaura coupling reactions (Churches & Hutton, 2016). The situation has since changed because of the emergence of boron-based drugs that show unique modes of inhibition and activity against various biological and biochemical targets (Barker et al., 2009; Smoum et al., 2012). Boron containing compounds exhibit unique biological properties and have been found to be generally nontoxic (Barker et al., 2009). Replacement of covalent carbon-carbon bonds with boron-nitrogen bonds has in many cases provided compounds with significantly improved biological and electronic properties. Moreover, the boron center can be converted from neutral trigonal planar (sp^2) to tetrahedral (sp^3) hybridization under proper physiological conditions to form strong interactions with the receptor (Özçayan, 2019). Previous studies on the 2,1-borazaronaphthalenes, for example, have demonstrated strong correlation of their biological properties *in vitro* as inhibitors of phosphodiesterase 10A (PDE10A) (Vlasceanu et al., 2015) and β_2 receptor (Rombouts et al., 2015) compared to the reference standards used for the assays. Benzodiazaborine scaffolds, on the other hand, serve as hydrophobic arene mimics (C=C versus B–N bond) in a biological context (Barker et al., 2009; Davis et al., 1998; Liu et al., 2009). The athranilamide moiety in the case of the 2-aryl-2,3-dihydrobenzodiazaborinin-4(1*H*)-one (azaborininone) scaffolds (**A**) shown in Figure 1 has been used extensively as a protecting group in the cross-coupling reactions, and also as an *ortho*-directing group in the *o*-C–H functionalization reactions to afford complex arylboronic acid derivatives that would be difficult to synthesize otherwise (Ihara et al., 2011). Although several methods for the synthesis of the 1,3,2-diazaboracyclohexane structures (**A**) have been described in the literature (Davies et al., 2017; Settepani, et al. 1970; Wang et al., 2019), only a few examples of these compounds and their *N*-substituted derivatives have previously been evaluated for biological activity particularly as insect chemosterilants, and were found to exhibit significant sterilizing activities against the house flies, *Musca domestica* L., compared to the corresponding benzeneboronic acids (Settepani et al., 1970). The molecular construct of these azaborininones resembles that of the 2-arylquinazolin-4(3*H*)-ones

(B) or their 2,3-dihydroquinazolin-4(1*H*)-one derivatives (C), which exhibit a wide range of biological and pharmacological properties as anti-virus, anti-bacterial, anti-inflammatory, anti-cancer, anti-allergic, anti-fungal, anti-rheumatic, anti-convulsant, and central nervous system (CNS) depressant activities (Hemalatha & Mahumitha, 2016). The 2-arylquinazolin-4(3*H*)-ones (Javaid et al., 2015; Wei et al., 2017) and the 2,3-dihydroquinazolin-4(1*H*)-ones (Barmak et al., 2019) have received extended attention as new classes of α -glucosidase inhibitors, which complements the activity of the pancreatic α -amylase. α -Amylase plays an important role in the early breakdown of complex carbohydrates such as large starch and glycogen molecules into simple absorbable disaccharides and polysaccharides (Dan et al., 2019; Imran et al., 2017; Rafique et al., 2020a). These sugars are, in turn, converted into glucose by α -glucosidase present in the brush border surface membrane of the intestinal cells for the absorption into the blood stream in the small intestine (Alqahtani, et al. 2020). This process results in an increased level of glucose in blood (hyperglycemia), which is a primary indication for diabetes mellitus (T2DM). Chronic hyperglycemia may result in oxidative stress due to the interaction of scavenger receptors, such as RAGE, with advanced glycoxidation end-products (AGEs) formed from the non-enzymatic glycation of proteins, lipids and nucleic acids with reducing sugars and with the products of glucose metabolism and their oxidation products (Chetan et al., 2015). Inhibition of α -glucosidase and/or α -amylase represents an effective strategy for the treatment of T2DM to suppress carbohydrate digestion and delay glucose uptake to lead to reduced blood sugar levels (Alqahtani et al., 2020; Rafique, et al. 2020b; Vieira et al., 2019). T2DM has become a serious global health concern and in the absence of adequate interventions, this metabolic disorder may lead to death or complications such as stroke, coronary heart disease or cancer (Rafique et al., 2020b; Tangvarasittichai, 2015). Most of the complications associated with diabetes have been found to result from free radical-mediated oxidative stress, due to the ability of free radicals to damage every class of biological macromolecules, including proteins, lipids, carbohydrates and nucleic acids (Rani et al., 2019). Targeting and inhibiting the activities of the enzymes implicated in the pathogenesis and/or progression of T2DM such as α -amylase and/or α -glucosidase as well as oxidative stress is considered to represent the most effective therapeutic strategy for the treatment of this metabolic disorder compared to combination therapies (Rafique et al., 2020a).

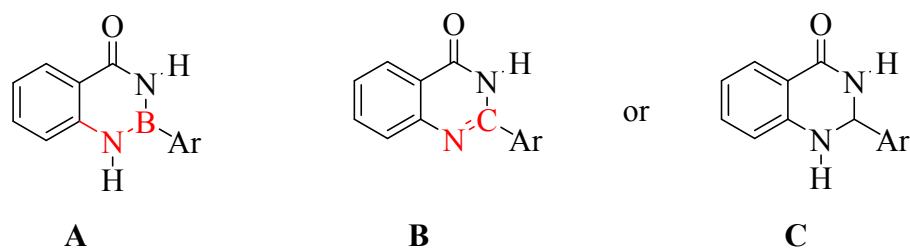


Figure 1: Azaborininone (**A**), quinazolin-4(*3H*)-one (**B**) and 2,3-dihydroquinazolin-4(*1H*)-one (**C**) scaffolds.

The replacement of C=C bond with isoelectronic B–N bonds has received considerable attention since the synthesis of 1,2-azaborine in 2008 and, this strategy is being explored for applications of organoboron derivatives in pharmaceutical and material science (Dixit et al., 2017). We considered the structural resemblance of the 1,3,2-diazaboracyclohexane derivatives **A** to those of quinoline-4-ones **B**, which have been found to inhibit α -glucosidase activity *in vitro*, and decided to synthesize these boron-based heterocycles. The main aim was to evaluate them through enzymatic assays *in vitro* for inhibitory effect against α -glucosidase and α -amylase activities. Due to the effects of oxidative stress on the induction of diabetic complications (Dixit et al., 2017; Rafique et al., 2020b; Tangvarasittichai, 2015) and considering the good antioxidant activities of boric acid esters and arylboronic acid derivatives (König et al., 1988), we also evaluated the test compounds for antioxidant potential through the 2,2-diphenyl-1-picrylhydrazyl (DPPH) and the nitric oxide (NO) free radical scavenging assays. Kinetic studies have been performed on the most active derivative against α -glucosidase and α -amylase complemented with molecular docking (*in silico*) to determine plausible protein–ligand interactions on a molecular level. Their ADME (absorption, distribution, metabolism, and excretion) properties have also been simulated to establish their drug-likeness at theoretical level. Since metabolic diseases require a stable long-term therapy, well tolerated and low toxicity, the test compounds were also assayed for toxicity against the African green monkey kidney (Vero) cells to establish their safety profile *in vitro*. Moreover, their potential antiproliferative effect was assayed against the human lung cancer (A549) cell line.

2. Materials and Methods

2.1. General considerations

The melting point values of the test compounds were recorded on a Thermocouple digital melting point apparatus (Mettler Toledo LLC, Columbus, OH, USA). The infrared (IR) spectra were recorded using the thin-film method on a Bruker VERTEX 70 FT-IR Spectrometer (Bruker Optics, Billerica, MA, USA) equipped with an ATR (diamond attenuated total reflectance) accessory. Merck kieselgel 60 (0.063–0.200 mm) (Merck KGaA, Frankfurt, Germany) was used as a stationary phase for column chromatography. The ^1H -NMR and ^{13}C -NMR spectra of the prepared compounds were obtained as dimethyl sulfoxide- d_6 (DMSO- d_6) solutions using Agilent 500 MHz NMR spectrometer (Agilent Technologies, Oxford, UK) operating at 500 MHz and 125 MHz for ^1H and ^{13}C , respectively. The chemical shifts are quoted relative to tetramethylsilane (TMS) used as an internal reference standard ($\delta = 0.00$ ppm) or to residual protonated solvent. The high-resolution mass spectra were recorded at an ionization potential of 70 eV using Micromass Autospec-TOF (double focusing high resolution) instrument (Waters Corp., Milford, MA, USA). α -Glucosidase type 1 from baker's yeast (G5003), *p*-nitrophenyl- α -D-glucopyranoside (N1377) and acarbose (A8980) were purchased from Sigma Aldrich (Pty) Ltd. (Modderfontein, Johannesburg, South Africa). α -Amylase inhibitor screening kit was sourced from Biovision via Biocom Africa (Pty) Ltd (Centurion, Pretoria, South Africa).

2.2. Typical procedure for the synthesis of the 1,3,2-diazaboracyclohexane derivatives **2a–j**

A stirred mixture of anthranilamide derivative **1** (1 equiv.), phenylboronic acid derivative (1 equiv.) and *p*-toluenesulfonic acid (0.1% equiv.) in toluene was refluxed for 2 h under Dean-Stark water collector conditions. The mixture was concentrated under reduced pressure and the solid obtained was filtered, washed with cold water and recrystallized from ethyl acetate to afford **2**. Compounds **2a–j** below were prepared in this fashion.

2-Phenyl-2,3-dihydrobenzo[*d*][1,3,2]diazaborinin-4(1*H*)-one (**2a**)

White solid (0.55 g, 85%), mp. 209–210 °C (Lit. 206–208 °C (Davies et al., 2017), 212–213 (Wang et al., 2019), 210–211 °C (Chissick et al., 1961)); ν_{max} (ATR) 686, 747, 1257, 1485, 1612, 1634, 3244, 3335 cm^{-1} ; ^1H -NMR (DMSO- d_6) 7.11 (1H, t, $J = 7.5$ Hz, H-7), 7.42–7.49 (4H, m, Ar), 7.57 (1H, dt, $J = 1.5$ and 8.5 Hz, H-6), 8.04–8.08 (3H, m, Ar), 9.34 (1H, s, NH), 9.72 (1H, s, NH); ^{13}C -NMR (DMSO- d_6) 120.8, 121.4, 123.4, 130.4, 130.6, 133.1, 134.9, 135.9, 136.0, 148.1, 169.0; HRMS (ES): m/z [M + H] $^+$ calc for $\text{C}_{13}\text{H}_{12}\text{BN}_2\text{O}$: 223.1043; found 223.1044.

2-(4-Fluorophenyl)-2,3-dihydrobenzo[*d*][1,3,2]diazaborinin-4(1*H*)-one (**2b**)

White solid (0.45 g, 65%), mp. 252–254 °C (Lit. 252–253 °C (Wang et al., 2019)); ν_{max} (ATR) 630, 692, 821, 1336, 1488, 1612, 1638, 3331, 3406 cm^{-1} ; ^1H -NMR (DMSO- d_6) 7.08 (1H t, $J = 7.5$

Hz, H-6), 7.40 (1H, d, $J = 7.5$ Hz, H-8), 7.62 (2H, t, $J = 8.5$ Hz, H-3',5'), 7.55 (1H, t, $J = 7.5$ Hz, H-5), 8.02 (1H, d, $J = 8.0$ Hz, H-5), 8.17 (2H, dt, $J = 5.7$ Hz and $J = 7.5$ Hz, H-2',6'), 9.32 (1H, s, NH), 9.73 (1H, s, NH); ^{13}C -NMR (DMSO- d_6) 115.2 (d, $^2J_{\text{CF}} = 19.9$ Hz), 118.6, 119.2, 121.4, 119.2, 121.3, 128.4, 129.0, 133.8, 136.3 (d, $^3J_{\text{CF}} = 7.6$ Hz), 145.9, 164.4 (d, $^1J_{\text{CF}} = 246.6$ Hz), 166.8; HRMS (ES): m/z $[\text{M} + \text{H}]^+$ calc for $\text{C}_{13}\text{H}_{11}\text{BFN}_2\text{O}$: 241.0948; found 241.0956.

2-(4-Chlorophenyl)-2,3-dihydrobenzo[d][1,3,2]diazaborinin-4(1*H*)-one (**2c**)

White solid (0.67 g, 77%), mp. 255–257 °C (Lit. 156–157 °C (Wang et al., 2019)); ν_{max} (ATR) 692, 722, 813, 1335, 1488, 1612, 1635, 3307, 3406 cm^{-1} ; ^1H -NMR (DMSO- d_6) 7.09 (1H, t, $J = 8.0$ Hz, H-6), 7.40 (1H, d, $J = 8.0$ Hz, H-8), 7.50 (2H, $J = 8.0$ Hz, H-3',5'), 7.55 (1H, dt, $J = 1.5$ and 8.5 Hz, H-5), 8.00 (1H, d, $J = 7.5$ Hz, H-5), 8.05 (2H, d, $J = 8.5$ Hz, H-2',6'), 9.36 (1H, s, NH), 9.74 (1H, s, NH); ^{13}C -NMR (DMSO- d_6) 118.6, 119.3, 121.4, 128.3, 128.4, 131.5, 133.9, 135.7, 136.1, 145.8, 166.7; HRMS (ES): m/z $[\text{M} + \text{H}]^+$ calc for $\text{C}_{13}\text{H}_{11}\text{BClN}_2\text{O}$: 257.0653; found 257.0653.

2-(4-Methoxyphenyl)-2,3-dihydrobenzo[d][1,3,2]diazaborinin-4(1*H*)-one (**2d**)

White solid (0.79 g, 82%), mp. 232–234 °C (Lit. 230.1–233.3 °C (Kamio et al., 2018)); ν_{max} (ATR) 752, 1179, 1273, 1569, 1640, 3299, 3359 cm^{-1} ; ^1H -NMR (DMSO- d_6) 3.79 (3H, s, -OCH₃), 6.99 (2H, d, $J = 8.5$ Hz, H-3',5'), 7.07 (1H, t, $J = \text{Hz}$, H-6), 7.41 (1H, d, $J = 8.0$ Hz, H-8), 7.54 (1H, dt, $J = 1.5$ and 8.5 Hz, H-7), 8.01 (1H, d, $J = 8.5$ Hz, H-4), 8.03 (2H, d, $J = 8.5$ Hz, H-2',6'), 9.19 (1H, s, NH), 9.61 (1H, s, NH); ^{13}C -NMR (DMSO- d_6) 55.4, 118.5, 119.1, 121.0, 124.0, 28.4, 133.8, 135.5, 146.1, 161.8, 166.8; HRMS (ES): m/z $[\text{M} + \text{H}]^+$ calc for $\text{C}_{14}\text{H}_{14}\text{BN}_2\text{O}_2$: 253.1148; found 253.1148.

2-(4-Hydroxyphenyl)-2,3-dihydrobenzo[d][1,3,2]diazaborinin-4(1*H*)-one (**2e**)

White solid (0.88 g, 85%), mp. 242–243 °C (Lit. 232.8–236.6 °C (Kamio et al., 2018)); ν_{\max} (ATR) 529, 821, 1354, 1488, 1612, 1640, 3306, 3406 cm^{-1} ; $^1\text{H-NMR}$ (DMSO- d_6) 6.83 (2H, d, $J = 8.5$ Hz, H-2',6'), 7.05 (1H, t, $J = 7.5$ Hz, H-6), 7.40 (1H, d, $J = 8.5$ Hz, H-8), 7.52 (1H, dt, $J = 1.5$ and 8.5 Hz, H-7), 7.90 (2H, d, $J = 8.0$ Hz, H-3',5'), 8.00 (1H, d, $J = 7.5$ Hz, H-5), 9.11 (1H, s, NH), 9.51 (1H, s, NH), 9.73 (1H, s, OH); $^{13}\text{C-NMR}$ (DMSO- d_6) 115.4, 118.4, 119.0, 120.9, 122.3, 128.4, 133.7, 135.6, 146.2, 160.2, 166.8. HRMS (ES): m/z $[\text{M} + \text{H}]^+$ calc for $\text{C}_{13}\text{H}_{12}\text{BN}_2\text{O}_2$: 239.0992; found: 239.0989.

6-Bromo-2-phenyl-2,3-dihydrobenzo[*d*][1,3,2]diazaborinin-4(1*H*)-one (2f)

White solid (1.02 g, 76%), mp. 275–278 °C (Lit. 282–284 °C (Yale, 1971)); ν_{\max} (ATR) 529, 670, 828, 1487, 1512, 1610, 1642, 3300, 3336 cm^{-1} ; $^1\text{H-NMR}$ (DMSO- d_6) 7.40 (1H, d, $J = 9.0$ Hz, H-8), 7.11–7.50 (3H, m, Ph), 7.70 (1H, dd, $J = 2.5$ and 9.0 Hz, H-7), 8.01 (2H, dd, $J = 1.5$ and 8.5 Hz, Ph), 8.06 (1H, d, $J = 2.5$ Hz, H-5), 9.43 (1H, s, NH), 9.84 (1H, s, NH); $^{13}\text{C-NMR}$ (DMSO- d_6) 112.9, 121.1, 127.8, 128.3, 130.4, 131.1, 132.3, 133.8, 134.5, 136.4, 145.1, 165.6; HRMS (ES): m/z $[\text{M} + \text{H}]^+$ calc for $\text{C}_{13}\text{H}_{11}\text{BBrN}_2\text{O}$: 301.0145; found 301.0148.

6-Bromo-2-(4-fluorophenyl)-2,3-dihydrobenzo[*d*][1,3,2]diazaborinin-4(1*H*)-one (2g)

White solid (0.99 g, 74%), mp. 301–302 °C; ν_{\max} (ATR) 530, 692, 1354, 1488, 1612, 1640, 3306, 3406 cm^{-1} ; $^1\text{H-NMR}$ (DMSO- d_6) 7.26 (2H, t, $J = 8.5$ Hz, H-2',6'), 7.36 (1H, d, $J = 8.5$ Hz, H-8), 7.69 (1H, dd, $J = 2.5$ and 9.0 Hz, H-7), 8.05 (1H, d, $J = 2.5$ Hz, H-5), 8.08 (2H, dt, $J = 5.7$ Hz and $J = 7.5$ Hz, H-3',5), 9.43 (1H, s, NH), 9.87 (1H, s, NH); $^{13}\text{C-NMR}$ (DMSO- d_6) 112.9, 115.3 (d, $^2J_{\text{CF}} = 19.9$ Hz), 120.9, 121.1, 128.6, 130.4, 136.3 (d, $^3J_{\text{CF}} = 7.6$ Hz), 136.4, 145.0, 154.5 (d, $^1J_{\text{CF}} = 246.5$ Hz), 165.6; HRMS (ES): m/z $[\text{M} + \text{H}]^+$ calc for $\text{C}_{13}\text{H}_{10}\text{BBrFN}_2\text{O}$: 319.0054; found 319.0054.

6-Bromo-2-(4-chlorophenyl)-2,3-dihydrobenzo[*d*][1,3,2]diazaborinin-4(1*H*)-one (2h)

White solid (0.56 g, 68%), mp. 261–263 °C; ν_{\max} (ATR) 530, 693, 722, 813, 1488, 1515, 1612, 1635, 3307, 3400 cm^{-1} ; $^1\text{H-NMR}$ (DMSO- d_6) 7.36 (1H, d, $J = 8.5$ Hz, H-8), 7.50 (2H, d, $J = 7.5$ Hz, H-2',6'), 7.70 (1H, dd, $J = 1.5$ and 8.5 Hz, H-7), 8.02 (2H, d, $J = 8.5$ Hz, H-3',5), 8.05 (1H, d, $J = 1.5$ Hz, H-5), 9.48 (1H, s, NH), 9.89 (1H, s, NH); $^{13}\text{C-NMR}$ (DMSO- d_6) 113.0, 121.0, 121.1, 128.4, 130.4, 135.7, 136.3, 136.5, 144.9, 165.5; HRMS (ES): m/z $[\text{M} + \text{H}]^+$ calc for $\text{C}_{13}\text{H}_{10}\text{BBrClN}_2\text{O}$: 334.9758; found 334.9745.

6-Bromo-2-(4-methoxyphenyl)-2,3-dihydrobenzo[*d*][1,3,2]diazaborinin-4(1*H*)-one (**2i**)

White solid (1.02 g, 85%), mp. 268–270 °C; ν_{\max} (ATR) 524, 720, 821, 1212, 1489, 1605, 1643, 3303, 3398 cm^{-1} ; $^1\text{H-NMR}$ (DMSO- d_6) 6.98 (2H, $J = 8.5$ Hz, H-3',5'), 7.37 (1H, d, $J = 8.5$ Hz, H-8), 7.68 (1H, dd, $J = 2.0$ and 8.5 Hz, H-7), 7.98 (2H, d, $J = 8.5$ Hz, H-2',6'), 8.04 (1H, d, $J = 2.0$ Hz, H-5), 9.31 (1H, s, NH), 9.75 (1H, s, NH); $^{13}\text{C-NMR}$ (DMSO- d_6) 55.5, 112.6, 113.9, 120.8, 121.0, 123.7, 130.4, 131.2, 135.6, 136.4, 145.2, 161.9, 165.2; HRMS (ES): m/z [M + H]⁺ calc for C₁₄H₁₃BBrN₂O₂: 331.0253; found 331.02490.

6-Bromo-2-(4-hydroxyphenyl)-2,3-dihydrobenzo[*d*][1,3,2]diazaborinin-4(1*H*)-one (**2j**)

White solid (1.23 g, 90%), mp. 315–317 °C; ν_{\max} (ATR) 529, 692, 821, 1213, 1354, 1487, 1611, 1642, 3304, 3406 cm^{-1} ; $^1\text{H-NMR}$ (DMSO- d_6) 6.81 (2H, d, $J = 7.5$ Hz, H-3',5'), 7.35 (1H, d, $J = 8.7$ Hz, H-8), 7.67 (2H, dd, $J = 1.2$ and 8.7 Hz, H-6), 7.87 (2H, d, $J = 7.5$ Hz, H-2',6'), 8.04 (1H, d, $J = 1.2$ Hz, H-5), 9.24 (1H, s, NH), 9.66 (1H, s, NH), 9.74 (1H, s, OH); $^{13}\text{C-NMR}$ (DMSO- d_6) 112.4, 115.4, 120.7, 120.9, 122.3, 130.4, 135.7, 136.3, 145.3, 160.4, 165.6; HRMS (ES): m/z [M + H]⁺ calc for C₁₃H₁₁BBrN₂O₂: 317.0097; found 317.0105.

2.3. Inhibition of α -glucosidase and α -amylase activity of **2a–j**

2.3.1. α -Glucosidase inhibitory activity assay of compounds **2a–j**

The α -glucosidase inhibitory activity of compounds **2a–j** was assayed following a method described in our previous study (Mphahlele et al., 2020). The stock solutions of the test compounds (100 μM) prepared in DMSO and acarbose as positive control in DMSO were diluted with 100 mM phosphate buffer to obtain the concentrations 1, 1.5, 5, 10, 25 and 50 μM . α -Glucosidase (0.96 U/mL) was diluted to 0.48 U/mL using a 100 mM phosphate buffer of pH 6.8. The enzyme (0.48 U/mL in 100 mM phosphate buffer of pH 6.8, 17 μL) was incubated with 17 μL of varying concentrations of the test compounds and acarbose as positive control in DMSO (1, 1.5, 5, 10, 25, 50 μM) at 37 °C for 10 min. Then 17 μL of 2 mM PNP-G was added to all the well containing reaction mixtures to initiate the reaction. Five different absorbance readings were recorded for each triplicate run at a wavelength of 400 nm using Varioskan flash microplate spectrophotometer (Thermo Scientific, Waltham, MA, USA). The concentrations of the compounds that inhibited 50% of α -glucosidase activity (IC_{50}) was determined by nonlinear regression analysis and expressed as the mean standard deviation (SD) of three distinct experiments using graph pad prism.

2.3.2. α -Amylase inhibitory activity assay of compounds **2a–j**

The α -amylase assay was performed in triplicate using a 96-well plate following the manufacturer's protocol as outlined in the α -Amylase Inhibitor Screening Kit (Catalog No. K482; Bio Vision). The stock solution (100 μ M) of the test compounds (**2a–j**), specific α -amylase inhibitor from *Triticum aestivum* included in the kit and acarbose were prepared in DMSO, and further diluted with α -amylase assay buffer to obtain final concentrations of 1, 1.5, 5, 10, 25 and 50 μ M. α -Amylase inhibitor from *Triticum aestivum* (10 μ L) and assay buffer (40 μ L) were added to 3 wells of the 96-well microplate to represent inhibitor control. The assay buffer (50 μ L) was added to the other three wells to represent the enzyme control. The test compounds (50 μ L) were added to the remaining designated wells of the plate. A solution of α -amylase enzyme (50 μ L) prepared by adding 490 μ L of assay buffer to 10 μ L of α -amylase enzyme was added to each of the wells containing the reaction mixture to initiate the reaction. The plate was incubated for 10 minutes at room temperature in the dark. Five different absorbance readings were recorded for each triplicate run at a wavelength of 405 nm using Varioskan flash microplate spectrophotometer (Thermo Scientific, Waltham, MA, USA). The IC_{50} and SD values were calculated using graph pad prism.

2.4. Kinetic studies on **2e** against α -glucosidase and α -amylase

2.4.1. Kinetic study on **2e** against α -glucosidase

The kinetics study on **2e** was performed according to the reaction conditions in 2.3.1 with inhibitor concentrations of 1, 1.5, 5, 10 μ M and the ranges of final substrate concentrations of 0.5–10 μ M. The type of inhibition was determined using Lineweaver-Burk plot (the inverse of velocity ($1/v$) against the inverse of the substrate concentration ($1/[S]$). The inhibitor constant was obtained by Dixon plot of the inverse of velocity ($1/v$) against concentration of inhibitor at each substrate concentration.

2.4.2. Kinetic study on **2e** against α -amylase.

Compound **2e** was selected for the kinetic study with various substrate concentrations of 0.5–1.5 μ M following the experimental conditions outlined in 2.3.2. The selected inhibitor concentrations were 5, 10, 25 and 50 μ M. The type of inhibition was determined by using Lineweaver-Burk plot and the inhibitor constant was obtained by Dixon plot (Cengiz et al., 2010).

2.5. 2,2-Diphenyl-1-picrylhydrazyl (DPPH) free radical scavenging assays of **2a–j**

The DPPH radical scavenging activity of the test compounds **2a–j** was evaluated by following a literature method described in our previous study (Mphahlele et al., 2020). Briefly the test compounds and ascorbic acid at various concentrations (1, 5, 10, 25, 50 and 100 μ M) in

DMSO were mixed with a solution of DPPH (0.20 mM) in methanol and incubated in the dark for 45 min. Five absorbance readings were recorded at 512 nm using Varioskan flash microplate spectrophotometer reader. The average values obtained from the absorbance readings were used to determine the IC₅₀ and standard deviation values.

2.6. Nitric oxide radical scavenging activity of compounds **2a–j**

Nitric oxide was generated from sodium nitroprusside and measured by Griess' reaction following the literature method using ascorbic acid as a positive control (Mohana, & Kumar, 2013). A mixture of sodium nitroprusside (10 mM), phosphate buffer saline and Griess reagent (1.00 g of sulphanic acid + 0.10 g naphthylethylene diamine dihydrochloride). Sodium nitroprusside (20 µL), phosphate buffer (5 µL) and the test compound (5 µL) were incubated at 25 °C for 2.5 h. After incubation, 20 µL of Griess reagent was added to the previous mixture and allowed to stand for 30 min. The absorbance of the colour developed during diazotization of nitrite with sulphanilamide and its subsequent coupling with naphthylethylenediamine hydrochloride. Five absorbance readings were recorded at 550 nm using Varioskan flash microplate spectrophotometer. The average values obtained from the absorbance readings of the triplicate runs were used to determine the IC₅₀ and standard deviation values.

2.7. Cytotoxicity Studies Using the MTT Assay

Cytotoxicity was measured in treated human lung cancer (A549) and African green monkey kidney (Vero) cell lines using the standard 3-[4,5-dimethylthiazol-2-yl]-2,5-diphenyltetrazolium bromide (MTT) assay. 10 000 cells per well (100 µL) were seeded in a 96-well microtiter plates and incubated for 24 h at 37 °C and 5% CO₂ to allow the cells to attach to the bottom of the wells. The cells were treated with compound concentrations ranging from 0–50 µM. The microtitre plates were further incubated for 24 h. After the 24 h incubation period, the MTT reagent (10 µL) was added to a final concentration of 0.5 mg/mL and the plate was further incubated for another 4 h. After 4 h, 100 µL of DMSO was added to each well and the plate was allowed to stand for 20 minutes to dissolve the tetrazolium salts. Absorbance readings were measured at 570 nm using the Varioskan Flash plate reader (Thermo Fisher Waltham, Massachusetts, USA).

2.8. Molecular docking studies of **2a–j** against α -glucosidase

The structures of α -glucosidase and α -amylase were obtained from RCSB PDB with accession number 5NN8 (Roig-Zamboni et al., 2017) and 5E0F, respectively. The polar hydrogen atoms of the proteins were added using AutoDockTools (Morris et al., 2009). The Kollman-Amber united atom partial charges and solvation parameters were then assigned using AutoDockTools. The

initial structure of the test compounds **2a–j** were prepared using Avogadro (Hanwell et al., 2012). The polar hydrogen atoms of the test compounds were retained while the Gasteiger charges and torsional angles were added using AutoDockTools. The grid box was centered at -12.000, -35.000, 88.000 (x, y z coordinates) for α -glucosidase and, -7.000, 10.000, -21.000 (x, y z coordinates) for α -amylase with $50 \times 50 \times 50$ points and 0.375 Å as grid spacing. Prior to docking calculation, the boron atom was replaced with carbon atom as boron parameters are not validated in Autodock4 (Morris et al., 2009). A total of 100 docking runs was performed using Lamarckian genetic algorithm employed in AutoDock4.2.6 (Morris et al., 2009) together with the following parameters: 2,500,000 energy evaluation, 27,000 generation, 150 population, 0.8 crossover rate and 0.02 mutation rate. The conformation in the most populated cluster with most favourable binding free energy was used for further interaction analysis.

2.9. Drug likeliness prediction of test compounds

The drug likeliness and pharmacokinetic properties of compounds **2a–j** were calculated using Molinspiration (www.molinspiration.com).

3. Results and Discussion

3.1. Chemical synthesis and characterization

The synthesis of the test compounds **2a–e** and **2f–j** was achieved via cyclocondensation-dehydration of anthranilamide derivatives **1a** (R = H) and **1b** (R = Br) with arylboronic acids in the presence of *p*-toluenesulfonic acid as catalyst in toluene under Dean-Stark conditions as represented in Scheme 1. The compounds were isolated by filtration without evidence of any side products, recrystallized from ethyl acetate, and then characterised using a combination of NMR, IR and high-resolution mass spectroscopic techniques. Crystals of quality suitable for X-ray diffraction were obtained for **2e**, and the molecular structure of these 1,3,2-diazaboracyclohexane derivatives was distinctly confirmed by X-ray diffraction. The crystallographic numbering has been used in the context of the X-ray analysis and it differs from systematic numbering for this class of compounds. The asymmetric unit shows molecules of **2e** held in chains via intermolecular hydrogen bonding interaction between the hydroxyl oxygen atom (O-H) of one molecule and hydrogen atom of N-H or C(O)N-H of the adjacent molecules (Figure 2). The molecular construct is essentially planar with a slight twist of the 2-phenyl group from the coplanarity of the

inhibitory effect *in vitro* against α -glucosidase and α -amylase activities, and for free radical scavenging properties as described in the next section.

3.2. Biological evaluation

3.2.1. Inhibitory effect on α -glucosidase and α -amylase, as well as antioxidant activity of **2a–j**.

Enzyme inhibitors have become of special interest in drug design and discovery because altering the activity of an enzyme has immediate and defined effects (Copeland et al., 2007). Compounds **2a–j** were screened through enzymatic assays *in vitro* for inhibitory effect against α -glucosidase and α -amylase activities. The IC_{50} values (μ M) defined as the concentration of compound exhibiting 50% inhibition of enzyme activity represented in Table 1 below were calculated from log dose inhibition curves, and are expressed as means \pm standard deviation (SD) of three independent experiments. We employed α -glucosidase from *Saccharomyces cerevisiae*, which is generally used as a target protein for screening the activity of α -glucosidase inhibitors. The 2-phenyl substituted derivative **2a** exhibited significant inhibitory effect against α -glucosidase activity compared to acarbose ($IC_{50} = 1.12 \pm 0.003 \mu$ M) with an IC_{50} value of $2.72 \pm 0.024 \mu$ M. The presence of a moderately π -electron delocalizing 2-(4-fluorophenyl) group resulted in higher activity for **2b** ($IC_{50} = 1.73 \pm 0.006 \mu$ M) compared to **2c** ($IC_{50} = 3.10 \pm 0.005 \mu$ M) substituted with a 4-chlorophenyl group at the C-2 position. Compounds **2d** and **2e** substituted with the strongly π -electron delocalizing and more lipophilic methoxy or hydroxyl group at the *para* position of the 2-phenyl ring were found to be the most active against α -glucosidase within this series with IC_{50} values of $1.15 \pm 0.013 \mu$ M and $1.35 \pm 0.005 \mu$ M, respectively. The presence of bromine atom at the C-6 position of the azaborininone scaffold resulted in relatively reduced α -glucosidase inhibitory effect for compounds **2f** and **2g** with IC_{50} values of $3.24 \pm 0.009 \mu$ M and $3.68 \pm 0.003 \mu$ M, respectively. However, a combination of the electron withdrawing bromine and 2-(4-chlorophenyl) substituent on the framework of **2h** resulted in significant inhibitory effect against α -glucosidase with an IC_{50} value of $2.09 \pm 0.005 \mu$ M. The presence of bromine at the C-6 position of compounds **2i** and **2j** also resulted in reduced inhibitory effect against α -glucosidase activity. α -Glucosidase inhibitors are also targeted by medicinal chemists for the treatment of other carbohydrate mediated diseases such as cancer, human immunodeficiency virus (HIV) and virus infection, and obesity (Gamblin et al., 2009).

α -Amylase inhibitory assay was carried out following protocol enclosed in BioVision's α -Amylase Inhibitor Screening kit (Catalog # K482-100) against acarbose ($IC_{50} = 11.71 \pm 0.051 \mu$ M) as a reference standard. The compounds within the two series of analogues showed varying degree

of α -amylase inhibitory activities with IC_{50} values in the range $2.66 \pm 0.056 \mu\text{M}$ to $28.14 \pm 0.010 \mu\text{M}$ (**2a–e**) and $5.12 \pm 0.036 \mu\text{M}$ to $23.42 \pm 0.032 \mu\text{M}$ (**2f–j**). The 2-phenyl substituted derivative **2a** exhibited increased activity against this enzyme with an IC_{50} value of $4.77 \pm 0.011 \mu\text{M}$, which is comparable to that of the reference standard. Compound **2b** which exhibited increased inhibitory effect against α -glucosidase was found to be less active against α -amylase with an IC_{50} value of $28.14 \pm 0.010 \mu\text{M}$. However, the 2-(4-chlorophenyl) analogue **2c** with moderate activity against α -glucosidase was found to be relatively more active against α -amylase than **2b** with an IC_{50} value of $11.15 \pm 0.062 \mu\text{M}$. The presence of a strongly π -electron delocalizing methoxy group at the *para* position of the 2-phenyl substituent resulted in increased activity for **2d** against α -amylase with an IC_{50} value of $10.41 \pm 0.027 \mu\text{M}$. Compound **2e** substituted with a strongly hydrogen bonding hydroxyl group at the *para* position of the 2-phenyl ring was found to be the most active derivative among the test compounds against α -amylase with an IC_{50} value of $2.66 \pm 0.056 \mu\text{M}$. Compounds **2d** and **2e** exhibit dual inhibitory effect against α -glucosidase and α -amylase activities, and these compounds have potential to suppress carbohydrate digestion and delay glucose uptake to lead to reduced blood sugar levels.

A combination of bromine atom at the C-5 position and 2-phenyl group in **2f** or a 2-(4-chlorophenyl) group in **2h** resulted in significantly reduced activity for these compounds compared with IC_{50} values of $23.05 \pm 0.023 \mu\text{M}$ and $23.42 \pm 0.032 \mu\text{M}$, respectively. These 6-bromo substituted derivatives are less active against this enzyme compared to their C-6 unsubstituted precursors **2a** and **2c**. However, a combination of the 6-bromo atom and 2-(4-fluorophenyl) group resulted in significantly increased activity for **2g** ($IC_{50} = 11.74 \pm 0.090 \mu\text{M}$) compared to **2b**. The most active compounds within the 6-bromo substituted series **2f–j** are **2i** and **2j** substituted with the lipophilic and strongly π -electron delocalizing methoxy or hydroxyl group at the *para* position of the 2-phenyl ring with IC_{50} values of $5.81 \pm 0.082 \mu\text{M}$ and $5.12 \pm 0.036 \mu\text{M}$, respectively. These oxygen-based substituents are capable of forming non-covalent interactions such as hydrogen and/or halogen bonds with protein residues of the receptor. Compounds **2b**, **2f** and **2h** with significantly reduced activity against α -amylase and significant inhibitory effect against α -glucosidase could serve as first-line drugs for the treatment of T2DM to prevent the digestion of carbohydrates in the intestine and defer glucose absorption, in turn, suppress post-prandial hyperglycaemia (PPHG). The other derivatives in both series have potential to serve as dual inhibitors of both carbohydrate hydrolysing enzymes to delay the glucose absorption and lower the postprandial blood glucose level.

Laboratory studies have revealed that a compound exhibiting a higher glucose-lowering effect also has good antioxidant properties (Famuyiwa, et al. 2019; Rafique et al., 2020b; Rani, et al., 2019) As a prelude to organoboron-based 6-membered heterocycles with dual carbohydrate hydrolysing inhibitory and antioxidant activities, the test compounds were evaluated for antioxidant properties through the DPPH and NO free radical scavenging assays with ascorbic acid as a reference standard (IC_{50} values of $9.25 \pm 0.003 \mu\text{M}$ and $7.40 \pm 0.019 \mu\text{M}$, respectively) for the assays. Within the series **2a–e**, only compounds **2a** and **2b** exhibited reduced DPPH scavenging activity compared to ascorbic acid with IC_{50} values of $28.81 \pm 0.002 \mu\text{M}$ and $36.42 \pm 0.013 \mu\text{M}$, respectively. However, both compounds exhibited increased NO scavenging activity compared to the reference standard with IC_{50} values of $5.16 \pm 0.050 \mu\text{M}$ and $2.73 \pm 0.027 \mu\text{M}$, respectively. Compound **2a** exhibited significant α -glucosidase and increased α -amylase inhibitory activities as well as NO scavenging activity. The presence of a 4-chlorophenyl group on the scaffold of **2c**, on the other hand, resulted in increased antioxidant activity in the DPPH assay, but moderate NO scavenging activity with IC_{50} values of $2.11 \pm 0.003 \mu\text{M}$ and $13.19 \pm 0.090 \mu\text{M}$, respectively. Increased antioxidant activity was also observed for **2d** substituted with a strongly π -electron delocalizing 4-methoxyphenyl group at position 2, and the corresponding IC_{50} values are $0.28 \pm 0.006 \mu\text{M}$ and $2.09 \pm 0.024 \mu\text{M}$ in the DPPH and NO radical scavenging assays, respectively. Increased propensity for the phenolic group to donate a hydrogen atom to the DPPH radical also resulted in increased free radical scavenging effect for **2e** (IC_{50} value of $0.36 \pm 0.003 \mu\text{M}$). This compound exhibited the highest NO scavenging activity in this series with an IC_{50} value of $0.45 \pm 0.019 \mu\text{M}$. The phenyl derivative **2f** within the 6-bromo substituted series **2f–j** exhibited relatively reduced antioxidant activity in both assays with IC_{50} values of $19.84 \pm 0.006 \mu\text{M}$ and $24.4 \pm 0.030 \mu\text{M}$, respectively. A combination of the 6-bromo atom and 2-(4-fluorophenyl) group in **2g**, on the other hand, resulted in increased DPPH ($IC_{50} = 4.67 \pm 0.017 \mu\text{M}$) and NO ($IC_{50} = 7.27 \pm 0.009 \mu\text{M}$) radical scavenging activity compared to ascorbic acid. The presence of bromine atom at C-6 position of compounds **2h**, **2i** and **2j** also resulted in increased antioxidant activity in both assays compared to the reference standard.

Considering that metabolic diseases require a stable long-term treatment, well tolerated and low toxicity, the test compounds were assayed for toxicity against the African green monkey kidney (Vero) cells through the 3-(4,5-dimethylthiazol-2-yl)-2,5-diphenyltetrazolium (MTT) assay to establish their safety profile at least *in vitro*. The MTT assay revealed that the test compounds were not toxic to the African green monkey kidney (Vero) cells after 24 h (refer to Fig. S2 of SI).

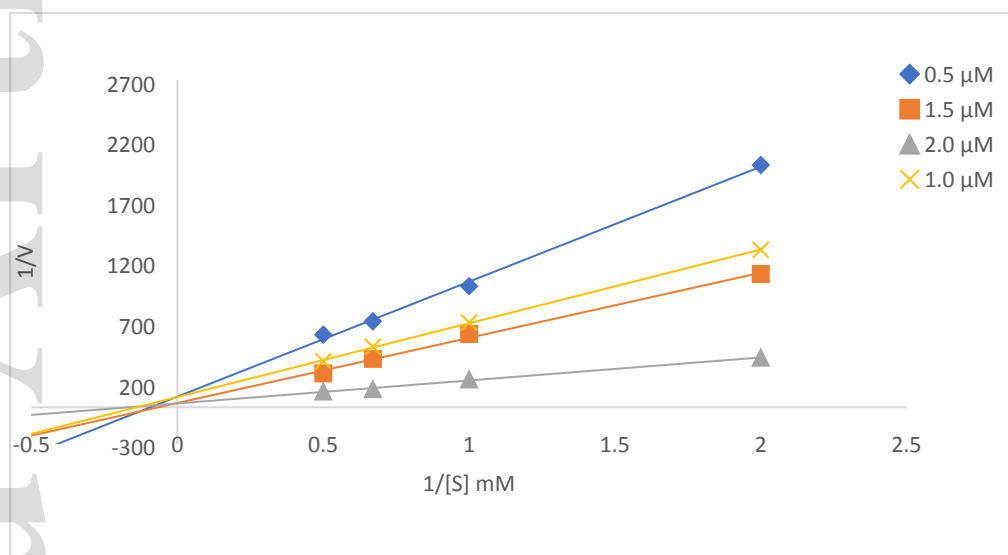
The Vero cells continue to be routinely used as a part of screening programs to evaluate the toxicity of compounds of different nature, either chemical or microbial toxins (Menezes et al., 2013). Additionally, increased glucose metabolism plays an important role in supporting cancer cell proliferation (Vander Heiden, et al. 2009), and therefore compounds that alter glucose metabolism are important candidates to be tested for anti-cancer properties. Consequently, compounds were assayed for cytotoxicity against the human lung cancer (A549) cell line as a representative model to establish their antiproliferative properties and selectivity between the normal and cancer cells. The preliminary cytotoxicity assay revealed that these compounds have little or no effect on the viability of A549 cell line. However, these preliminary cytotoxicity results require further tests on different cell lines to confirm further the safety of these compounds. Compound **2e** with dual inhibitory activity against α -glucosidase and α -amylase was selected for mechanism-based enzyme inhibition studies as described in the next section.

Table 1: Inhibition of **2a–j** on α -glucosidase and α -amylase, and their free radical scavenging potential.

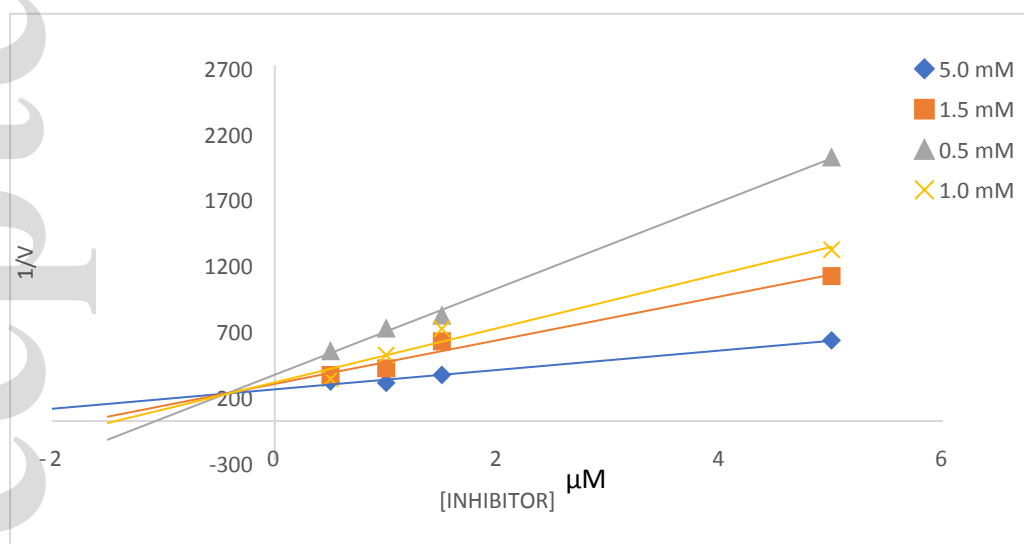
2a–l	R	Ar	IC₅₀ (μM, SD)			
			α-Glucosidase	α-Amylase	DPPH	NO
2a	H	C ₆ H ₅ -	2.72 \pm 0.024	4.77 \pm 0.11	28.81 \pm 0.002	5.16 \pm 0.05
2b	H	4-FC ₆ H ₄ -	1.73 \pm 0.006	28.14 \pm 0.01	36.42 \pm 0.013	2.73 \pm 0.03
2c	H	4-ClC ₆ H ₄ -	3.10 \pm 0.005	11.15 \pm 0.06	2.11 \pm 0.003	13.19 \pm 0.09
2d	H	4-MeOC ₆ H ₄ -	1.15 \pm 0.013	10.41 \pm 0.03	0.28 \pm 0.006	2.09 \pm 0.02
2e	H	4-HOC ₆ H ₄ -	1.35 \pm 0.005	2.66 \pm 0.06	0.36 \pm 0.003	0.45 \pm 0.02
2f	Br	C ₆ H ₅ -	3.24 \pm 0.009	23.05 \pm 0.02	19.84 \pm 0.006	24.4 \pm 0.03
2g	Br	4-FC ₆ H ₄ -	3.68 \pm 0.003	11.74 \pm 0.09	4.67 \pm 0.017	7.27 \pm 0.01
2h	Br	4-ClC ₆ H ₄ -	2.09 \pm 0.005	23.42 \pm 0.03	14.4 \pm 0.017	8.12 \pm 0.05
2i	Br	4-MeOC ₆ H ₄ -	4.08 \pm 0.017	5.81 \pm 0.08	5.14 \pm 0.006	10.48 \pm 0.02
2j	Br	4-HOC ₆ H ₄ -	4.44 \pm 0.005	5.12 \pm 0.04	6.43 \pm 0.004	6.01 \pm 0.01
Acarbose	-	-	1.12 \pm 0.003	11.71 \pm 0.05	-	-
Ascorbic acid	-	-	-	-	9.25 \pm 0.003	7.40 \pm 0.02

3.2.2 Kinetic study

The Lineweaver-Burk plot of $1/V$ versus $1/[S]$ in the presence of different concentrations of compound **2e** in the case of α -glucosidase gave a series of straight lines that intersect on the x-axis (Figure 3a). The plot shows an unchanged Michaelis constant (K_m) value as the velocity of the reaction (V_{max}) increases. The Dixon plot (Figure 3b) has straight lines that intersect above the x-axis with the calculated K_i value of $0.42 \pm 0.11 \mu\text{M}$. The observed trends are consistent with a mixed mode of inhibition of this compound against α -glucosidase activity.



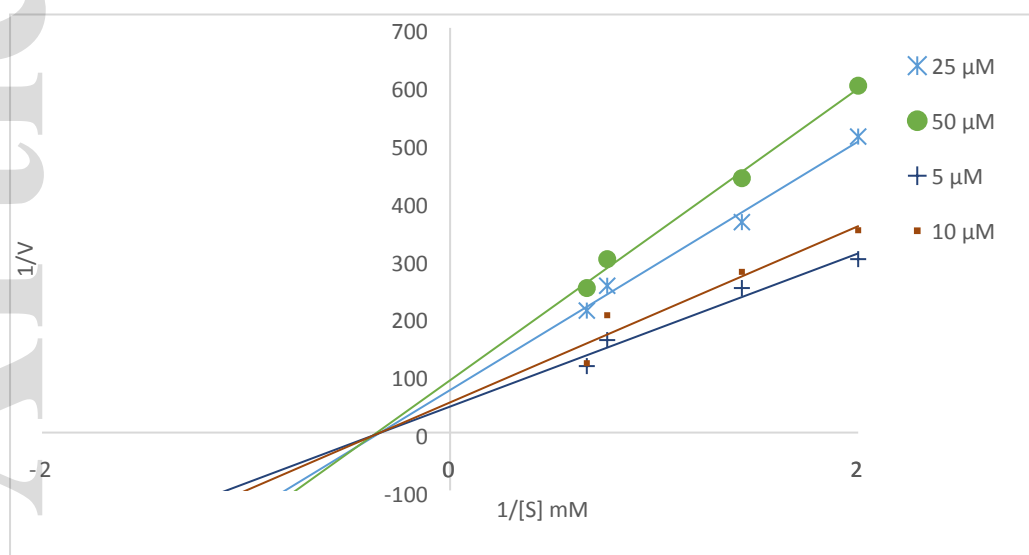
(a)



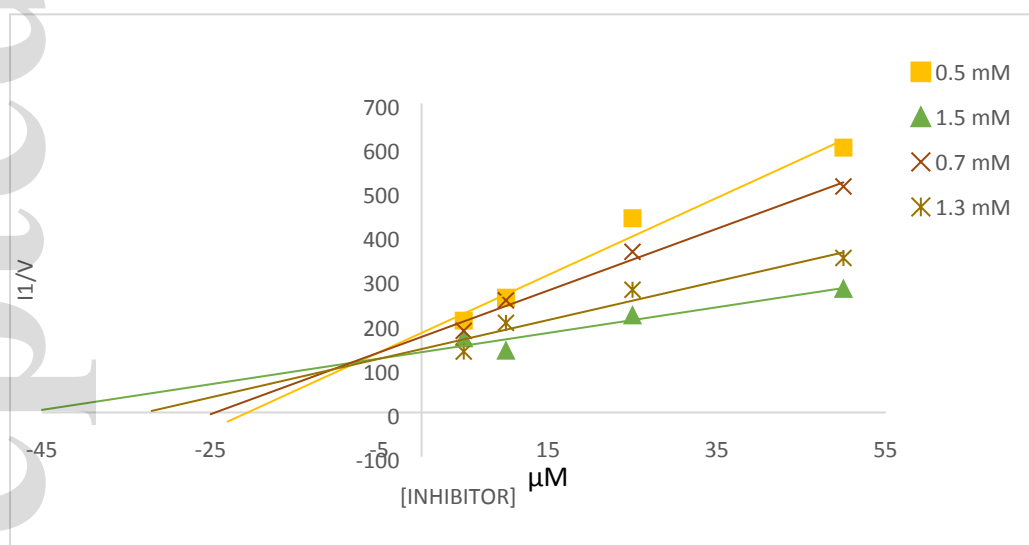
(b)

Figure 3: Lineweaver-Burk plot (a) and Dixon plot (b) of **2e** against α -glucosidase.

The Lineweaver-Burk plot of **2e** (Figure 4a) is characterised by decreasing V_{\max} (0.023–0.013 $\mu\text{M}/\text{min}$) and an unchanged K_m value of 3.00. Its Dixon plot (Figure 4b), shows several straight lines that intersect above the x-axis with a K_i value of $5.22 \pm 0.23 \mu\text{M}$. The observed trends are consistent with a mixed mode of inhibition of this compound against α -amylase activity. This compound probably binds to the active site and other sites of the enzyme to affect its activity.



(a)



(b)

Figure 4: Lineweaver-Burk plot (a) and Dixon plot (b) of **2e** against α -amylase.

We speculated that the N-H, C=O, -OH and OCH_3 , halogen atoms, and the π -electrons of the aromatic rings in these compounds may have hydrophobic effects, hydrogen bonded salt bridges, electrostatic interactions, π -stacking interactions, and other noncovalent bonds with the amino acid

residues of the target enzymes. Consequently, we subjected these compounds to molecular docking (*in silico*) studies to determine plausible protein–ligand interactions on a molecular level, and to establish their drug likeness at theoretical level.

3.2.3 Molecular docking into α -glucosidase and α -amylase active sites

The test compounds were docked into the active sites of α -glucosidase (PDB code: 5NN8) and α -amylase (PDB code: 5E0F). The conformation in the most populated cluster with most favourable free binding energy (BE) was used for further interaction analysis (refer to Table S1 in SI for BE values). The most active derivative **2e** from series **2a–e** against both enzymes, and compound **2h** from series **2f–j** which exhibited significant activity against α -glucosidase and reduced inhibitory effect against α -amylase were chosen as representative models for the docking poses into α -glucosidase (Figure 5) and α -amylase (Figure 6) active sites. Both **2e** and **2h** form three hydrogen bonds with α -glucosidase. Three hydrophobic contacts and a π -cation interaction are also predicted between **2e** and α -glucosidase. Compound **2h**, on the other hand, has five hydrophobic contacts that support it in the binding pocket of α -glucosidase.

The favourable binding affinity of **2e** against α -amylase could be contributed by the hydroxyl group of the phenol region which forms as many as four hydrogen bonds with the protein residues in the active site of this enzyme. Two hydrogen bonds are also predicted to form between the azaborininone region of **2e** with α -amylase. The azaborininone region of **2h** make the same number of hydrogen bond with α -amylase while the bromine atom forms two halogen bonds with α -amylase Arg195. Both **2e** and **2h** form hydrophobic contacts with the residues Trp58, Trp59 and Tyr62, and the two compounds are also involved in π - π stacking interaction with Tyr62.

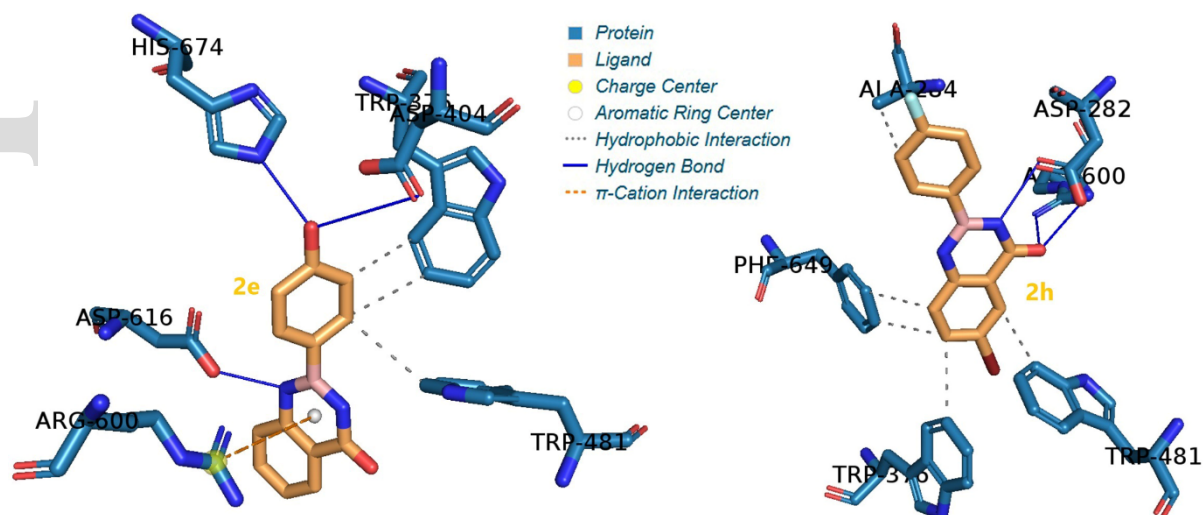


Figure 5. The interaction analysis between compound **2e** and **2h** with α -glucosidase.

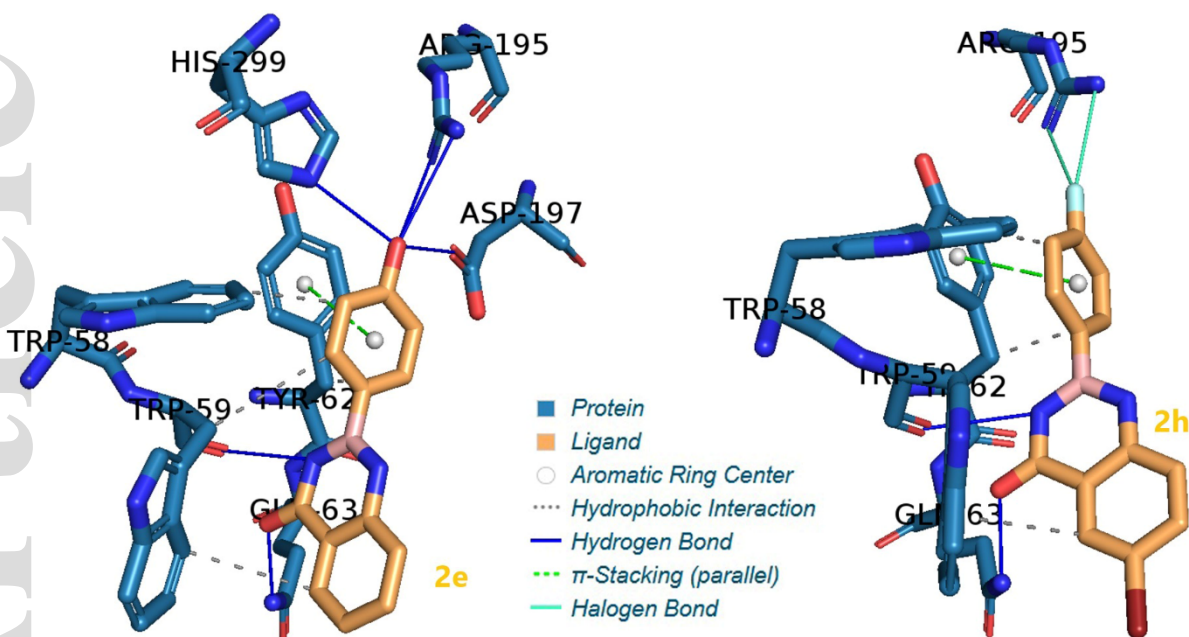


Figure 6. The interaction analysis between compound **2e** and **2h** with α -amylase.

3.2.4 Drug-likeness predictions

The drug-likeness of the test compounds was predicted at theoretical level through the Lipinski rule of five which states that for a molecule to act as a therapeutic candidate it must possess four characteristics, which are (i) number of hydrogen bond donors should not be more than 5, number of hydrogen bond acceptors should not be more than 10, the molecular mass should be less than 500 Da, and LogP (octanol-water partition coefficient) should not be greater than 5 (Table 2). The test compounds fulfill all the four druglikeness characteristics (refer to Table S2 in SI). The predicted absorption rate of nearly 90% for the highest active derivative **2e** against both enzymes has also suggested possible oral administration for this compound.

4. Conclusions

The lipophilic and strongly π -electron delocalizing methoxy (**2d** and **2i**) or hydroxy (**2e** and **2j**) group increase the electron density of the these azaborininones, and therefore the ability of this scaffold to engage in hydrogen bonding and hydrophobic interactions with the protein residues in the receptor. Compounds **2d**, **2e**, **2i** and **2j** with dual inhibitory effect against α -glucosidase and α -amylase activities, and strong free radical scavenging activity have potential to serve as multi-target ligands to reduce blood sugar level and probably ameliorate complications associated with oxidative stress. These compounds showed little or no effect on the viability of A549 cell line and

were also not toxic to the Vero cells. These preliminary results support the potential of the 1,3,2-diazaboracyclohexane derivatives as bioisosteric replacements for the 2-arylquinazolin-4-ones in antidiabetic drug discovery programs. More analogues will be synthesised to optimize the inhibition effects of this 1,3,2-diazaboracyclohexane scaffold. Moreover, further cellular-based *in vitro* and *in vivo* studies including bioavailability and cell permeability would help to clarify the mechanism of action of these compounds in the body, and to establish their safety profile as potential multi-target agents against the pathogenesis and progression of T2DM. It is envisaged that the results of this study will offer medicinal chemists an opportunity to explore these carbonyl-bearing boron-heterocyclic scaffolds and their analogues for other modes of inhibition against a variety of biochemical and biological targets, and pioneer new areas of drug discovery.

Supplementary Information: Figure S1: Copies of the ^1H - and ^{13}C -NMR spectra of compounds **2a–j**; Table S1: Estimated binding free energy obtained from docking simulation of compound **2a–j** towards α -glucosidase (PDB id 5NN8) and α -amylase (PDB id 5E0F); Table S2. The pharmacokinetics properties predictions of test compounds **2a–j**; and Fig. S2. Cytotoxicity results of compounds **2a–j** against A549 and Vero cell lines.

Author Contributions: Conceptualization, M.J.M.; Methodology, data curation and analyses, M.J.M.; bioassays, NMM & STJ; Writing–review & editing, M.J.M. and Y.S.C.

Funding: This project was funded by the University of South Africa and the National Research Foundation (NRF) in South Africa (NRF GUN: 118554) as well as Universiti Sains Malaysia (RUi grant: 1001/CIPPM/8011051). The views and opinions expressed herein are those of the authors and not of the funding bodies.

Data Availability Statement: The CIF file containing complete information on the studied structure was deposited with the Cambridge Crystallographic Data Center, CCDC 2032015, and is freely available upon request from the following website: www.ccdc.cam.ac.uk/datarequest/cif or by contacting the Cambridge Crystallographic Data Centre, 12, Union Road, Cambridge CB2 1EZ, UK; fax: +44-1223-336033; email: deposit@ccdc.cam.ac.uk.

Acknowledgements: We are grateful to the University of Stellenbosch Central Analytical Facility (CAF) and the University of the Witwatersrand for mass spectrometric and X-ray data, respectively.

Conflict of interest: The authors declare no conflict of interest.

References

- Alqahtani, A. S., Hidayathulla, S., Rehman, M. T., ElGamal, A. A., Al-Massarani, S., Razmovski-Naumovski, V., Alqahtani, M. S., El Dib, R. A., & AlAjmi, M. F. (2020). Alpha-amylase and alpha-glucosidase enzyme inhibition and antioxidant potential of 3-oxolupenal and katononic acid isolated from *Nuxia oppositifolia*. *Biomolecules*, 10, 61. DOI:10.3390/biom10010061.
- Barker, S. J., Ding, C. Z., Akama, T., Zhang, Y. -K., Hernandez, V., & Xia, Y. (2009). Therapeutic potential of boron-containing compounds. *Future Medicinal Chemistry*, 1, 1275–1288. DOI:10.4155/fmc.09.71.
- Barmak, A., Niknam, K., & Mohebbi, G. (2019). Synthesis, structural studies, and α -glucosidase inhibitory, antidiabetic, and antioxidant activities of 2,3-dihydroquinazolin-4(1*H*)-ones derived from pyrazol-4-carbaldehyde and anilines. *ACS Omega*, 4, 18087–18099. DOI:10.1021/acsomega.9b01906.
- Carpenter, R. D., Natarajan, A., Lau, E. Y., Andrei, M., Solano, D. M., Lightstone, F. C., DeNardo, S. J., Lam, K. S., & Kurth, M. J. (2010). Halogenated benzimidazole carboxamides target integrin $\alpha_4\beta_1$ on T-cell and B-cell lymphomas. *Cancer Research*, 70, 5448–5456. DOI:10.1158/0008-5472.
- Cengiz, S., Cavas, L., & Yurdakoc, K. (2010). Alpha-amylase inhibition kinetics by caulerpenyne. *Mediterranean Marine Science*, 93–103. DOI:10.12681/mms.93.
- Chetan, S., Amarjeet, K., Thind, S. S., Baljit, S., & Shiveta, R. (2015). Advanced glycation End-products (AGEs): An emerging concern for processed food industries. *Journal of Food Science and Technology*, 52, 7561–7576. DOI:10.1007/s13197-015-1851-y.
- Chissick, S. S., Dewar, M. J. S., & Maitlis, P. M. (1961). New heteroaromatic compounds. XIV. Boron-containing analogs of purine, quinazoline and perimidine. *Journal of the American Chemical Society*, 83, 2708–2711. DOI:10.1021/ja01473a025.
- Churches, Q. I., & Hutton, C. A. (2016). Introduction, interconversion and removal of boron protecting groups. *ACS Symposium Series*, 1236, 357–377. DOI:10.1021/bk-2016-1236.ch011.
- Copeland, R. A., Harpel, M. R., & Tummino, P. J. (2007). Targeting enzyme inhibitors in drug discovery. *Expert Opinion on Therapeutic Targets*, 11, 967–978. DOI:10.1517/14728222.11.7.967.

- Dan, W. -J., Zhang, Q., Zhang, F., Wang, W. -W., & Gao, J- M. (2019). Benzonate derivatives of acetophenone as potent α -glucosidase inhibitors: synthesis, structure–activity relationship and mechanism. *Journal of Enzyme Inhibition and Medicinal Chemistry*, 34, 937–945. DOI:10.1080/14756366.2019.1604519.
- Davies, G. H. M., Mukhtar, A., Saeednia, B., Sherafat, F., Kelly, C. B., & Molander, G. A. (2017). Azaborininones: Synthesis and structural analysis of a carbonyl containing class of azaborine. *Journal of Organic Chemistry*, 82, 5380–5390. DOI:10.1021/acs.joc.7b00747.
- Davis, M. C., Franzblau, S. G., & Martin, A. R. (1998). Syntheses and evaluation of benzodiazaborine compounds against *M. tuberculosis* H₃₇R_v *in vitro*. *Bioorganic & Medicinal Chemistry Letters*, 8, 843–846.
- Dixit, V.A., Goundry, W. R. F., & Tomasi, S. (2017). C=C/B–N substitution in five membered heterocycles. A computational analysis. *New Journal of Chemistry*, 41, 3619–3633. DOI:10.1039/C7NJ00950J.
- Famuyiwa, S. O., Sanusi, K., Faloye, K. O., Yilmaz, Y., & Ceylan, Ü. (2019). Antidiabetic and antioxidant activities: Is there any link between them? *New Journal of Chemistry*, 43, 13326–13329. DOI:10.1039/C9NJ01251F.
- Gamblin, D. P., Scanlan, E. M., & Davis, B. G. (2009). Glycoprotein synthesis: An update. *Chemical Reviews*, 109, 131–163. DOI:10.1021/cr078291i.
- Hanwell, M. D., Curtis, D. E., Lonie, D. C., Vandermeersch, T., Zurek, E., & Hutchison, G. R. (2012). Avogadro: An advanced semantic chemical editor, visualization, and analysis platform. *Journal of Cheminformatics*, 4, 17. <http://www.jcheminf.com/content/4/1/1>.
- Hemalatha, K., & Madhumitha, G. (2016). Synthetic strategy with representation on mechanistic pathway for the therapeutic applications of dihydroquinazolinones. *European Journal of Medicinal Chemistry*, 123, 596–630. DOI:10.1016/j.ejmech.2016.08.001.
- Ihara, H., Koyanagi, M., & Suginom, M. (2011). Anthranilamide: A Simple, removable ortho-directing modifier for arylboronic acids serving also as a protecting group in cross-coupling reactions. *Organic Letters*, 13, 2662–2665. DOI:10.1021/ol200764g.
- Imran, S., Taha, M., Selvaraj, M., Ismail, N. H., Chigurupati, S., & Mohammad, J. I. (2017). Synthesis and biological evaluation of indole derivatives as α -amylase inhibitor. *Bioorganic Chemistry*, 73, 121–127. DOI:10.1016/j.bioorg.2017.06.007.
- Javid, K., Saad, S. M., Rasheed, S., Moin, T., Sued, N., Fatima, I., Salar, U., Khan, K. M. Perveen, S., & Choudhary, M. I. (2015). 2-Arylquinazolin-4(3*H*)-ones: A new class of α -

- glucosidase inhibitors. *Bioorganic Chemistry* 23, 7417–7421. DOI:10.1016/j.bmc.2015.10.038.
- Kamio, S., Kageyuki, I., Osaka, I., Hatano, S., Abe, M., & Yoshida, H. (2018). Anthranilamide (aam)-substituted diboron: palladium-catalyzed selective B(aam) transfer. *Chemical Communication*, 54, 9290–9293. DOI:10.1039/c8cc05645e.
- König, T., Mannel, D., Häbicher, W. D., & Schwertlick, K. (1988). Organoboron antioxidants: Part 1—Boric acid derivatives as primary antioxidants. *Polymer Degradation and Stability*, 22, 137–145. DOI:10.1016/0141-3910(88)90037-7.
- Liu, L., Marwitz, A. J. V., Matthews, B. W., & Liu, S. -Y (2009). Boron mimetics: 1,2-Dihydro-1,2-azaborines bind inside a nonpolar cavity of T4 lysozyme. *Angewandte Chemie International Edition*, 48, 6817–6819. DOI:10.1002/anie.200903390.
- Menezes, C., Valério, E., & Dias, E. (2013). The kidney Vero-E6 cell line: A suitable model to study the toxicity of microcystins. In *New Sights into Toxicity and Drug Testing*, Vol. 2. Rijeka, Croatia: InTechOpen, pp. 29–48. DOI:10.5772/54463.
- Mohana, K.N., & Kumar, C. B. P. (2013). Synthesis and antioxidant activity of 2-amino-5-methylthiazol derivatives containing 1,3,4-oxadiazole-2-thiol moiety. *ISRN Organic Chemistry*, 8, 620718. DOI:10.1155/2013/620718.
- Morris, G. M., Huey, R., Lindstrom, W., Sanner, M. F., Belew, R. K., Goodsell, D. S., & Olson. A. J. (2009). AutoDock4 and AutoDockTools4: Automated docking with selective receptor flexibility. *Journal of Computational Chemistry*, 40, 2785–2791. DOI:10.1002/jcc.21256.
- Mphahlele, M. J., Magwaza, N. M., Gildenhuis, S., & Setshedi, I. B. (2020). Synthesis, α -glucosidase inhibition and antioxidant activity of the 7-carbo-substituted 5-bromo-3-methylindazoles. *Bioorganic Chemistry*, 97, 103702. DOI:10.1016/j.bioorg.2020.103702.
- Özçayan, G. (2019). Synthesis of organoboron amide-ester branched derivatives of poly(itaconic anhydride-alt-2-vinyl-1,3-dioxolane) and cancer cells interaction studies. *Boron*, 4, 159–171. DOI:10.30728/boron.515517.
- Rafique, R., Khan, K. M., Arshia, Chigurupati, S., Wadood, A., Rehman, A. U., Salar, U., Venugopal, V., Shamim, S., Taha, M., & Perveen, P. (2020a). Synthesis, *in vitro* α -amylase inhibitory, and radicals (DPPH & ABTS) scavenging potentials of new *N*-sulfonohydrazide substituted indazoles. *Bioorganic Chemistry*, 94, 105410. DOI:10.1016/j.bioorg.2019.103410.

- Rafique, R., Khan, K. M., Arshia, Kanwal, Chigurapati, S., Wadood, A., Rehman, A. U., Karunanidhi, A., Hamed, S., Taha, M., & Al-Rashida, M. (2020b). Synthesis of new indazole based dual inhibitors of α -glucosidase and α -amylase enzymes, their *in vitro*, *in silico* and kinetics studies. *Bioorganic Chemistry*, 94, 103195. DOI:10.1016/j.bioorg.2019.103195.
- Rani, V., Deep, G., Singh, R. K., Palle, K., & Yadav, U. C. S. (2016). Oxidative stress and metabolic disorders: Pathogenesis and therapeutic strategies. *Life Sciences*, 1148, 183–193. DOI:10.1016/j.lfs.2016.02.002.
- Roig-Zamboni, V., Cobucci-Ponzano, B., Iacono, R., Ferrara, M. C., Germany, S., Bourne, Y., Parenti, G, Moracci, M., & Sulzenbacher, G. (2017). Structure of human lysosomal acid alpha-glucosidase– a guide for the treatment of Pompe disease. *Nature Communications*, 8, 1111. DOI:10.1038/s41467-017-01263-3.
- Rombouts, F. J. R., Tovar, F., Austin, N., Tresadern, G., & Trabanco, A. A. (2015). Benzazaborinines as novel bioisosteric replacements of naphthalene: Propranolol as an example. *Journal of Medicinal Chemistry*, 58, 9287–9295. DOI:10.1021/acs.jmedchem.5b01088.
- Settepani, J. A., Stokes, J. B., & Bokkovec, A. B. (1970). Insect chemosterilants. VIII. Boron compounds. *Journal of Medicinal Chemistry*, 13, 128–131. DOI:10.1021/jm00295a032.
- Smoum, R., Rubinstein, A., Dembitsky, V. M., & Srebnik, M. (2012) Boron containing compounds as protease inhibitors. *Chemical Reviews*, 112, 4156–4220. DOI:10.1021/cr608202m.
- Tangvarasittichai, S. (2015). Oxidative stress, insulin resistance, dyslipidemia and type 2 diabetes mellitus. *World Journal of Diabetes*, 6, 456–480. DOI:10.4239/wjd.v6.i3.456.
- Vander Heiden, M. G., Cantley, L. C., & Thompson, C. B. (2009). Understanding the Warburg effect: the metabolic requirements of cell proliferation. *Science*, 324, 1029–1033. DOI: 10.1126/science.1160809.
- Vieira, R., Souto, S. B., Sánchez-López, E., Machado, A. L., Severino, P., Jose, S., Santini, A., Fortuna, A., Garcia, M. L., Silva, A. M., & Souto, E. B. (2019). Sugar-lowering drugs for type 2 diabetes mellitus and metabolic syndrome– Review of classical and new compounds: Part-I. *Pharmaceuticals*, 12, 152. DOI:10.3390/ph12040152.

Vlasceanu, A., Jessing, M., & Kilburn, J. P. (2015) BN/CC isosterism in borazoranaphthalenes towards phosphodiesterase 10A (PDE10A) inhibitors. *Bioorganic & Medicinal Chemistry*, 23, 4453–4461. DOI:10.1016/j.bmc.2015.06.019.

Wang, H. -J., Zhang, M., Li, W. -J., Ni, Y., Lin, J., & Zhang, Z. -H. (2019). An efficient Ni/Pd catalyzed chemoselective synthesis of 1,3,2-benzodiazaborininones from boronic acids and anthranilamides. *Advanced Synthesis & Catalysis*, 361, 5018–5024. DOI: 10.1002/adsc.2019.

Wei, M., Chai, W. -M., Wang, R., Yang, Q., Deng, Z., & Peng, Y. (2017). Quinazolinone derivatives: Synthesis and comparison of inhibitory mechanisms on α -glucosidase. *Bioorganic & Medicinal Chemistry*, 25, 1303–1308. DOI:10.1016/j.bmc.2016.09.042.

Yale, H. L. (1971). Novel boron heterocycles. I. 2,3-dihydro-1,3,2-benzodiazaborin-4(1*H*)-ones and 1,2-dihydro-1,3,2-benzodiazaborines. *Journal of Heterocyclic Chemistry*, 8, 193–204. DOI:10.1002/jhet.5570080203.

Zhao, P., Nettleton, D. O., Karki, R. G., Zécari, F. J., & Liu, S. -L. (2017). Medicinal chemistry profiling of monocyclic 1,2-azaborine. *ChemMedChem*, 12, 358–361. DOI:10.1002/cmdc.201700047.